

**Large Variations In The Volatile Content Of Olivine-Hosted Melt Inclusions From Lunar Magmas.** M. Le Voyer<sup>1</sup>, E. H. Hauri<sup>1</sup> and A. E. Saal<sup>2</sup>, <sup>1</sup>Department of Terrestrial Magnetism, Carnegie Institution of Washington, 5241 Broad Branch Road, NW, Washington DC 20015-1305, <sup>2</sup>Department of Earth, Environmental & Planetary Sciences, Brown University, 324 Brook Street, Providence, RI, 02912.

**Introduction:** Recent studies have detected the presence of water and other volatiles in lunar magmas, at levels equivalent to those found on mid-ocean ridge basalts (MORB) [1-4], indicating a similar amount of volatiles in the depleted MORB mantle on Earth and in the lunar mantle. These results could potentially put strong bounds on the existing models of the Moon formation by giant impact and accretion of the ejected material, especially on the impact energy and the corresponding amount of devolatilization. In order to better constrain the range in volatile contents of the lunar mantle, we performed new analyses of volatile contents in olivine-hosted melt inclusions from A17 orange glass. The results show a range of variation that exceeds previously published values.

**Sample description and analytical methods:** We separated olivine grains from sample 74220, which is a picritic sample of pyroclastic origin. Olivines (0.1-1.0 mm in diameter) were selected for the presence of completely enclosed melt inclusions, and single olivine crystals were mounted individually in indium mounts and polished to expose new melt inclusions. The melt inclusions vary from 3-60  $\mu\text{m}$  diameter and have rounded or triangular shapes. They are mostly glassy but contain a variable amount of  $\mu\text{m}$ -scale dendrites formed during rapid quench, as well as a gas vesicle, similar to most terrestrial melt inclusions. We analyzed the volatile contents in the melt inclusions and the matrix glasses using the NanoSIMS Cameca 50L at the Department of Terrestrial Magnetism. After 60s of presputtering using a 30 x 30  $\mu\text{m}$  rastered beam, the analyses were performed using the "image" mode with a 10 nA primary current and a 10 x 10  $\mu\text{m}$  raster area. Images were then processed and regions of interest were selected using the software L'image, in order to exclude any potential area of contamination (bubble, crack, polishing pit, or host olivine) from the analysis.

**Results:** The melt inclusions contain 0.3-0.7 ppm C (equivalent to 1.1-2.5 ppm  $\text{CO}_2$ ), 1.5-5.3 ppm Cl, 171-1478 ppm  $\text{H}_2\text{O}$ , 30-109 ppm F and 274-967 ppm S (Fig.1). The associated matrix glasses contain lower volatiles contents (0.03-0.3 ppm Cl, 4-31 ppm  $\text{H}_2\text{O}$ , 6-20 ppm F and 255-626 ppm S, Fig. 1), with the exception of C (0.3-0.7 ppm, similar to the melt inclusions). The total range in the volatile contents of the melt inclusions represents a  $\sim 3$  fold increase in C, F, Cl and S and a  $\sim 9$  fold increase in  $\text{H}_2\text{O}$  (Fig. 1). Note that the measured C contents are low but significantly higher

than the detection level (0.1 ppm C, obtained from repeated measurements of Suprasil quartz glass under the same analytical conditions). The melt inclusion data reported here are similar to previously published data on lunar olivine-hosted melt inclusions with respect to their  $\text{H}_2\text{O}$  contents [2], but they show a much larger range that reaches higher F, Cl and S contents (Fig. 1).

**Processes responsible for the range in volatile contents of the melt inclusions:** Similarly to terrestrial magmas, numerous processes affect the volatile contents of lunar melts during magma evolution. First, as volatiles are incompatible in most silicate minerals typically found in basaltic samples, the melt will become enriched in volatiles during fractional crystallization. However, (i) the basaltic melt inclusions and matrix glasses studied here are relatively high-MgO [2], indicative of an early crystallization stage, (ii) we analyzed the melt inclusions by including both the glass and the dendrites in the 10 x 10 raster, which minimizes the effect of post-entrapment crystallization, and (iii) the entire range in volatile contents (up to a 9-fold increase in  $\text{H}_2\text{O}$ , Fig. 1) is too large to be solely due to the effect of fractional crystallization. Second, the fact that both the matrix glasses and the melt inclusions have similar C contents indicates that they have both lost their initial C through degassing. The presence of the vapor bubble in most melt inclusions also indicates the importance of the degassing process in controlling the volatile content of these melt inclusions. However, the  $\text{H}_2\text{O}$ , F, Cl and S contents recorded in the melt inclusions are significantly higher than those of the matrix glasses ( $\sim 70$ , 6, 20 and 2 times higher on average, respectively, Fig. 1), indicating that the melt inclusions have been significantly less affected by degassing compared to the matrix glasses. In this case, the melt inclusion with the highest volatile content is best representative of the undegassed primary melt. Finally, we find a linear co-variation in the volatile contents of the melt inclusions. This is especially true for F and Cl ( $R^2=0.9$ ), but is also statistically significant for any other pairs of volatiles (Fig. 1), with the exception of C. These trends could be explained by (i) a coupled degassing of  $\text{H}_2\text{O}$ , C, Cl and S, or (ii) a mixing process between volatile-poor and volatile-rich melts, most likely formed by variable degassing extents in separate regions of the same primary magma body. If we model such a mixing process by using the most volatile-rich

melt inclusion for the undegassed endmember and the most volatile-poor matrix glass for the degassed endmember, we see that the melt inclusions data fall along a mixing trend, with an amount of undegassed component varying between ~30% and ~70%. In reality, although the three processes described above (fractional crystallization, degassing and mixing) would all affect the volatile content of these melt inclusions, we infer that most of the range in volatile contents is caused by degassing, as this process would be the most effective in reproducing both the low C contents and the large range in other volatiles (up to 9-fold for H<sub>2</sub>O) recorded by the melt inclusions.

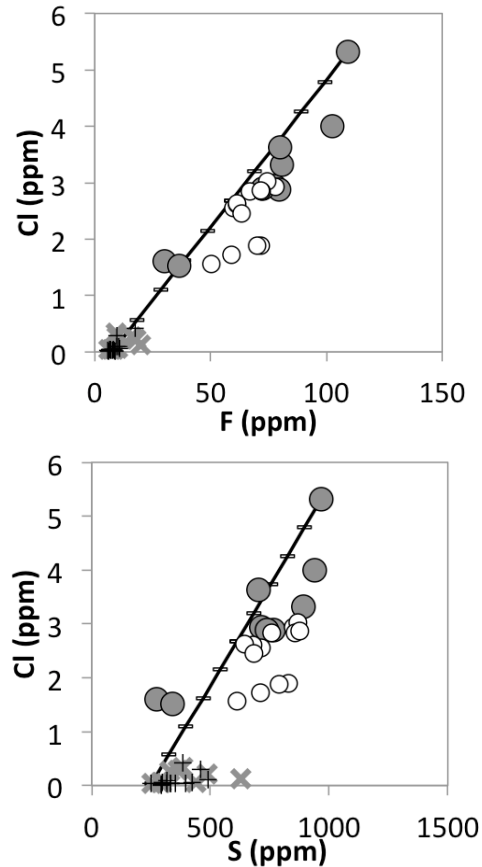
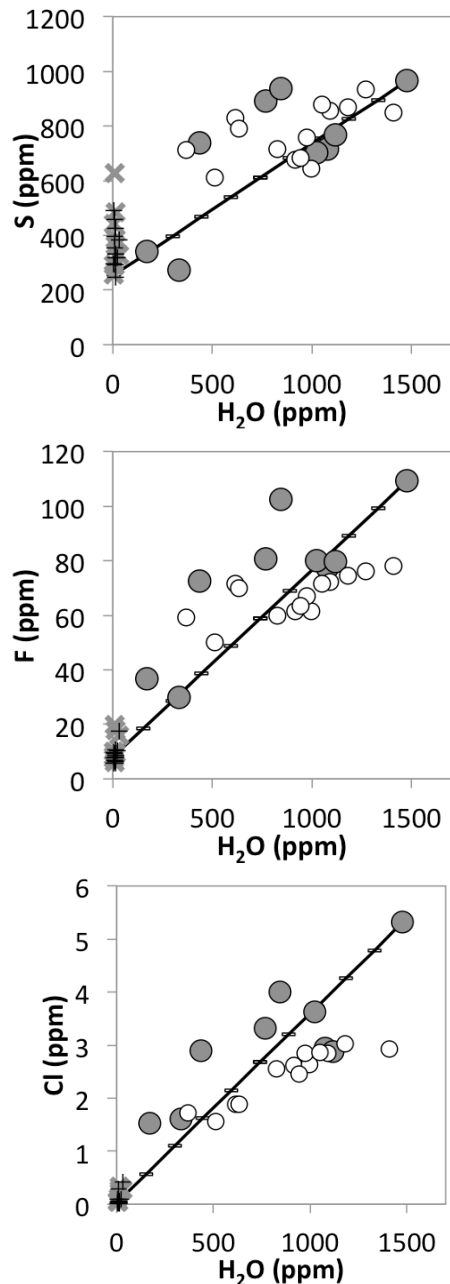


Figure 1: Variations in volatile element contents in the melt inclusions (circles) and matrix glasses (crosses) from A17 orange glass sample 74220. Grey symbols are from this study; others are from [2]. The line represents a mixing model between the most H<sub>2</sub>O-rich melt inclusion and the most H<sub>2</sub>O-poor matrix glass, where each graduation corresponds to a 10% increment in the mixing proportions.

**Volatile contents in the primary melts and source mantle:** In order to circumvent the effect of fractional crystallization, we can examine the systematics between volatile elements and non-volatile trace elements of similar incompatibility. By using the volatile contents of the least degassed melt inclusion from this study, and the average trace element of the melt inclusions from the same sample [2], we obtain estimates of 82 for H<sub>2</sub>O/Ce, 6.2 for F/Nd, 0.36 for Cl/Nb and 104 for S/Dy for the undegassed melt, which is ~1.3, 1.7, 2.2 and 1.1 times higher than previously reported for the undegassed primary melt of the A17 orange glass sample 74220 [2].

**References:** [1] Hauri E. H. et al. (2011) *Science* 333, 213-215. [2] Hauri, E.H., et al., (2015) *EPSL* 409 p. 252-264. [3] Saal A. E. et al. *Nature* 454, 192-195. [4] Saal A. E. et al. (2013) *Science* 340, 1317-1320.